The Astrophysical Journal, 875:130 (7pp), 2019 April 20 https://doi.org/10.3847/1538-4357/ab0e6f

Discovery of a Lyα-emitting Dark Cloud within the $z \sim 2.8$ SMM J02399-0136 System

Qiong Li[1], Zheng Cai[2,3,10], J. Xavier Prochaska[3,4], Fabrizio Arrigoni Battaia[5], R. J. Ivison[5,6], Edith Falgarone[7], Sebastiano Cantalupo[8], Mateusz Matuszewski[9], James Don Neill[9], Ran Wang[1], Chris Martin[9], and Anna Moore[9]
[1] Kavli Institute for Astronomy and Astrophysics, Peking University, Beijing 100871, People's Republic of China
[2] Tsinghua Center of Astrophysics & Department of Astronomy, Tsinghua University, Beijing 100084, People's Republic of China
[3] UCO/Lick Observatory, University of California, 1156 High Street, Santa Cruz, CA 95064, USA; zcai@ucolick.org
[4] Kavli Institute for the Physics and Mathematics of the Universe (Kavli IPMU; WPI), The University of Tokyo, 5-1-5 Kashiwanoha, Kashiwa, Chiba Prefecture 277-8583, Japan
[5] European Southern Observatory, Karl-Schwarzschild-Strasse 2, D-85748 Garching, Germany
[6] Institute for Astronomy, University of Edinburgh, Blackford Hill, Edinburgh EH9 3HJ, UK
[7] Laboratoire de Physique de l'ENS, ENS, Université PSL, CNRS, Sorbonne Université, Université Paris-Diderot, Paris, France
[8] Department of Physics, ETH Zurich, CH-8093 Zurich, Switzerland
[9] Cahill Center for Astrophysics, California Institute of Technology, 1216 East California Boulevard, Mail code 278-17, Pasadena, CA 91125, USA
Received 2018 April 9; revised 2019 March 6; accepted 2019 March 7; published 2019 April 23

Abstract

We present Keck/Keck Cosmic Web Imager (KCWI) integral field spectrograph observations of the complex system surrounding SMM J02399−0136 (a lensed $z = 2.8$ sub-mm galaxy), including an associated Lyα nebula, a dust-obscured, broad-absorption-line quasar, and neighboring galaxies. At a 3σ surface brightness contour of 1.6×10^{-17} erg s^{-1} cm^{-2} arcsec^{-2}, the Lyα nebula extends over 17 arcsec ($\gtrsim$140 physical kpc) and has a total Lyα luminosity of 2.5×10^{44} erg s^{-1} (uncorrected for lensing). The nebula exhibits a kinematic shear of $\sim$1000 km s^{-1} over 100 pkpc with lowest velocities east of SMM J02399−0136 and increasing to the southwest. We also discover a bright, Lyα emitter, separated spatially and kinematically from the nebula, at a projected separation of $\approx$60 kpc from the quasar. This source has no clear central counterpart in deep *Hubble Space Telescope* imaging, giving an intrinsic Lyα rest-frame equivalent width greater than 312 Å (5σ). We argue that this "dark cloud" is illuminated by the quasar with a UV flux that is orders of magnitude brighter than the emission along our sightline. This result confirms statistical inferences that luminous quasars at $z > 2$ emit UV radiation anisotropically. Future KCWI observations of other lines, e.g., Lyβ, He II, C IV, etc, and with polarimetry will further reveal the origin of the Lyα nebula and nature of the dark cloud.

Key words: cosmology: observations – galaxies: formation – galaxies: high-redshift – intergalactic medium – quasars: general

1. Introduction

In the unified model of active galactic nucleus (AGN) emission from Antonucci (1993), the ionizing radiation propagates anisotropically from an active black hole due to the absorption from a clumpy torus. For this reason, AGNs appear differently depending on their inclination with respect to our line of sight. This model thereby unifies observations of two main classes of AGNs: Type I quasars, which have both broad and narrow emission lines, and Type II quasars, which have only narrow lines (e.g., Tristram et al. 2007; Nenkova et al. 2008). Both types of AGNs are characterized by extreme ionizing luminosities (up to $\sim 10^{47}$ erg s^{-1}), which should reveal the surrounding gas distribution out to large distances, if illuminated (Rees 1988; Haiman & Rees 2001; Cantalupo et al.2005).

Following this idea, over the last few years, a few enormous Lyα nebulae (ELANe) with sizes up to 500 kpc were discovered around luminous Type I and a few Type II QSOs at $z = 2$–3 (e.g., Hennawi & Prochaska 2013; Cantalupo et al. 2014; Hennawi et al. 2015; Cai et al. 2017; Arrigoni Battaia et al. 2018). Moreover, deep narrow band (NB) imaging and Integral Field Spectroscopy have revealed the existence of Lyα line emitters with high equivalent width (EW$_0$ > 240 Å) around $z = 2$–3 quasars, also known as "dark galaxies" (e.g., Cantalupo et al. 2012; Marino et al. 2018). Overall, the simultaneous and detailed studies of the kinematics, metallicity, luminosity, and abundance of the ELANe and dark galaxies provide us an indispensable opportunity to understand the interactions between the galaxies hosting AGNs at high redshift and the gas that surrounds and fuels them (e.g., Prochaska & Hennawi 2009; Fumagalli et al. 2011).

With these motivations in mind, we have initiated a survey of $z > 2$ quasars and previously known Lyα nebulae with the Keck Cosmic Web Imager (KCWI; Morrissey et al. 2012), a new blue-sensitive integral field spectrograph with wavelength coverage spanning from $\sim$3500 to 5600 Å. Its field-of-view (FoV), spectral resolution, and capability for precise sky subtraction are optimal for studying gas on scales of $\approx$200 kpc. Here we report on deep KCWI observations of the complex system surrounding SMM J02399−0136 (Ivison et al. 1998), hereafter SMM J02399, the first galaxy selected at submm wavelengths (i.e., a SMG), gravitationally amplified by the massive foreground galaxy cluster A370. Typical SMGs are dust-rich and highly obscured. In particular, the Lyα nebula surrounding SMM J02399 was quickly found to lie at $z \sim 2.8$, using the 4 m Canada–France–Hawaii Telescope, in part because its Lyα luminosity is extremely bright ($\sim 10^{44}$ erg s^{-1}; Ivison et al. 1998). This source resides at the high luminosity end of the *WISE* detected LAB in Bridge et al. (2013), which are also Lyα nebulae powered by SMGs and have a Lyα luminosity of 10^{42}–10^{44} erg s^{-1}. It was the first SMG detected in CO, revealing it to contain a massive reservoir of molecular gas ($\approx 10^{11}$ $M_\odot$, Frayer et al. 1998). This gas reservoir was later shown to cover a large volume and contain multiple, merging galaxies (Ivison et al. 2010), one of which is a dusty, broad-absorption-line (BAL) quasar (Villar-Martín et al. 1999a, 1999b; Vernet & Cimatti 2001; Frayer et al. 2018, e.g., Genzel et al. 2003). The

[10] Hubble Fellow.

existence of a large reservoir of diffuse molecular gas has been recently inferred by observations of the CH^+ cation (E. Falgarone et al. 2019, in preparation), following the detections against several other SMGs (Falgarone et al. 2017).

Inspired by these earlier results, we observed the system with KCWI tuned to the Lyα nebula and directed to cover it and its neighboring galaxies and quasar. To our surprise, the data reveal a new, luminous Lyα source—the primary focus of this paper, which is structured as follows. We describe our KCWI observation and data reduction process in Section 2. In Section 3, we present the detection of the $\gtrsim$100 kpc Lyα nebula powered by this system and the discovery of a new dark cloud illuminated by the nearby BAL QSO. Finally, we discuss the Lyα nebula and the physical interpretations of the newly discovered dark galaxy in Section 4, and give a brief summary in Section 5. Throughout this paper, we assume a flat cosmological model with $\Omega_\Lambda = 0.7$, $\Omega_m = 0.3$ and $H_0 = 70\,\mathrm{km\,s^{-1}\,Mpc^{-1}}$, which implies the physical scale is $\approx$7.85 kpc per arcsec at the redshift of SMM J02399−0136. We follow the naming convention presented in Ivison et al. (2010): L1 marks the BAL quasar; L2 is a low-surface-brightness companion to the east of L1; L2SW is a massive, extremely luminous and dust-obscured starburst galaxy, east–south–east of L1 and south–west of L2; L1N is a faint, compact northern component, visible in post-SM2 *HST* imaging.

2. Observations and Data Reduction

2.1. KCWI Observations

The KCWI observations of SMM J02399 were carried out on UT 2017 October 21 (seeing $\sim$1.″5) using KCWI on the Keck II telescope of the W. M. Keck Observatory in Hawaii. We used the BM1 grating and the medium slicer (slice width $\sim$0.″7), which yields an IFU datacube with FoV of 20″ × 16.″8 (pixel scale of 0.″3 × 0.″7) centered on J023951.88−013558.0, the quasar optical position given by Ivison et al. (1998). The grating was tilted to give a central wavelength of 4620 Å and provides a spectral resolution, $R \approx 4000$. The good wavelength coverage is $\sim$4230–5010 Å. The total on-source exposure time is four 10-minute exposures, each dithered by $\sim$0.″6. For sky observations, we used an "offset-target-field" to construct the sky datacube. The offset-target has a different redshift and is located $\sim$2 degrees from SMM J02399. It is a compact point source at the Lyα wavelength of SMM J02399.

To convert the spectral images and calibration frames (arcs, flats, bias) to a calibrated datacube, we used the IDL-based KCWI data reduction pipeline.[11] Basic CCD reduction is performed on each science frame to obtain a bias-subtracted, cosmic-ray-cleaned, gain-corrected image. The continuum flat images are employed for CCD response corrections and pixel-to-pixel variations. We used a continuum-bar image and an arc image (ThAr) to define the geometric transformations and wavelength calibration, generating a rectified object datacube (see the pipeline documents[12]). Twilight flats were used for slice-to-slice flux correction, and the data was corrected for atmospheric refraction. Each object and sky frame was flux calibrated with the standard star, Hiltner 600. For the sky frame, we first masked the point source of the offset-target, and then estimated the sky level at each wavelength channel by the median of unmasked sky pixels. Then, for each channel, we subtract the sky from SMM J02399. For each exposure, we found the QSO centroid to measure the offsets between exposures, and then performed a weighted mean with inverse-square variance weighting to construct the final datacube.

2.2. Ancillary Data

CO(3–2) observations of SMM J02399 were obtained by Genzel et al. (2003) with a synthesized beam of 5.2 × 2.4 arcsec^2. We use these data, kindly provided by L. Tacconi, to compare the cool molecular gas emission with that traced by Lyα. SMM J02399 is strongly magnified by A370, which was imaged as part of the *HST* Frontier field survey (HST-14038, PI: J. Lotz). It was observed with three broadband filters: ACS/WFC F435W, F606W and F814W, for total exposure times of 12, 6 and 29 hr, respectively. We retrieved the publicly available reduced data[13] and produced an average image, weighted by the exposure time. The F435W filter covers the Lyα emission of SMM J02399 and thereby provides an independent estimate of its spatial extent.

3. Results

3.1. Deep NB Imaging at Lyα

Figure 1 shows our continuum-subtracted, pseudo-narrow band image, spanning $\approx$30 Å with central wavelength $\lambda_{\rm NB} = \lambda_{\rm Ly\alpha}(1 + z_{L1}) \approx 4025$ Å, and Gaussian smoothed spatially by 2″. The 3σ depth flux density of this image in a 1.7 arcsec^2 aperture[14] is $4 \times 10^{-18}\,\mathrm{erg\,s^{-1}\,cm^{-2}\,\AA^{-1}}$, corresponding to a surface brightness of $1.6 \times 10^{-17}\,\mathrm{erg\,s^{-1}\,cm^{-2}\,arcsec^{-2}}$. In the following discussion, we refer only to observed quantities (i.e., without lensing corrections for magnification by A370[15].) The peak surface brightness in the region encompassing L1 and L2 is $\approx 1.2 \times 10^{-16}\,\mathrm{erg\,s^{-1}\,cm^{-2}\,arcsec^{-2}}$. To a 3$\sigma$ surface brightness contour, this nebula has a lensing-uncorrected size of $\gtrsim$17 arcsec (i.e., $\gtrsim$140 physical kpc) and has a total Lyα luminosity of $2.5 \times 10^{44}\,\mathrm{erg\,s^{-1}}$.

Figure 1 also reveals a bright, previously unreported source approximately 7.″5 to the SW of L1. We refer to this source as L3 and measure a Lyα luminosity of $1.3 \times 10^{43}\,\mathrm{erg\,s^{-1}}$ within an aperture of 6 arcsec^2. The peak surface brightness of L3 is $3.0 \times 10^{-17}\,\mathrm{erg\,s^{-1}\,cm^{-2}\,arcsec^{-2}}$, similar to Ly$\alpha$ blobs surveyed by Matsuda et al. (2004, 2011), as well as the extended Lyα nebulae detected around $z \sim 2$ high-redshift radio galaxies and radio-loud quasars (e.g., Villar-Martín et al. 2007; Heckman et al. 1991). The properties for individual sources are listed in Table 1.

Figure 2(a) shows the *HST* imaging around L3, comprised of ACS/WFC F435W, F606W, and F814W deep images and contours for the CO and Lyα emission. CO(1–0) and CO(3–2) observations suggest there is a large gas reservoir in this system, and the peak location of which coincides with the Lyα emission at L1. We have also confirmed that there is no continuum (stellar) counterparts corresponding to L3 in the SDSS, *WISE* and 2MASS

[11] Available at https://github.com/kcwidev/kderp/releases/tag/v0.6.0.
[12] https://github.com/kcwidev/kderp/blob/master/AAAREADME
[13] http://archive.stsci.edu/
[14] In this paper, we used two kinds of apertures. One ($\sim$1.7 arcsec^2; 1.″4 × 1.″2) matches the seeing of the observations, and it is used to subtract spectral features and measure the continuum in the *HST* image. The second ($\sim$6 arcsec^2) is defined by the 5σ contour at the L3 location (see Figure 1) and is used to measure its total/average properties. This second aperture is used to calculate the observed (Section 3.1 para.2) and inferred results (in Section 4.1).
[15] The magnification factor of L1, L2, L3 are almost the same ($\sim$2.4× for each; Ivison et al. 2010).

Table 1
The Properties for Individual Source in SMM J02399

Source	R.A. J2000	Decl. J2000	$\lambda_{detected}$ Å	Redshift	Aperture	SB(Lyα) 10^{-17} ergs^{-1}cm^{-2}arcsec^{-2}	L(Lyα)[a] 10^{43} ergs^{-1}
(1)	(2)	(3)	(4)	(5)	(6)	(7)	(8)
L1	02:39:51.86	−01:35:58.15	4625.5	2.8048 ± 0.0004	∼0.″7 × 0.″6	8.3 ± 1.8	3.5 ± 0.6
L2	02:39:52.04	−01:35:57.27	4621.6	2.7985 ± 0.0004	∼0.″7 × 0.″6	8.3 ± 1.7	3.5 ± 0.6
L3	02:39:51.63	−01:36:04.56	4634.9	2.81259 ± 0.00008	∼1.″4 × 1.″2	3.0 ± 0.6	1.3 ± 0.2
Entire nebula							25.0 ± 3.6

Note.
[a] The observed luminosities, which do not include the lensing magnification factor of 2.4× due to the foreground cluster (Ivison et al. 2010).

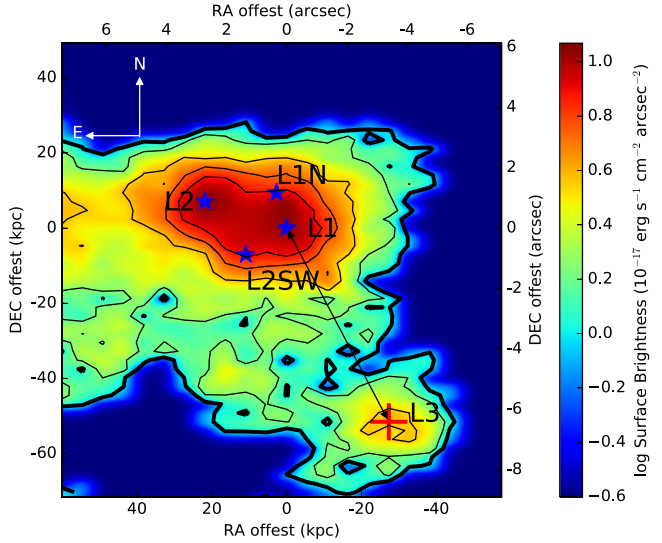

Figure 1. The continuum-subtracted pseudo-narrow band Lyα image of the gas surrounding SMM J02399. The color map and the contours indicate the Lyα flux density and the signal-to-noise ratio (+3, 5, 10, 15, 20σ), respectively. The axes are centered on the position of L1 and the image has been smoothed with a Gaussian kernel of 2″. The offset from L1 to L3 is 3.″45 W, 6.″45 S (∼58.8 kpc).

catalogs[16] , nor in the deeper surveys of PanSTARRS, DES, DECaLS.[17] Examining Figure 2(b), we derive a 5σ upper limit to the continuum $4.0 \pm 0.8 \times 10^{-20}$ erg s^{-1} cm^{-2} Å^{-1} from the *HST* F435W image in a 1.7 arcsec^2 aperture. The Lyα rest-frame equivalent width is therefore greater than 312 Å, which follows the scenario of a dark galaxy[18] illuminated by aluminous AGN (Cantalupo et al. 2012).

Here we also estimated the 5σ continuum upper limits from both F606W and F814W imaging in an aperture of 1.7 arcsec^2, obtaining 1.9×10^{-20} erg s^{-1} cm^{-2} Å^{-1} and 9.7×10^{-21} erg s^{-1} cm^{-2} Å^{-1}, respectively. Then we calculated that the 5σ upper limit of the rest-frame UV SFR is 0.3 yr^{-1} (Kennicutt & Evans 2012). This SFR is not high enough to give rise to the bright Lyα emission.

3.2. Lyα Kinematics

Our KCWI datacube enables a study of Lyα emission throughout the complex system surrounding SMM J02399. Figure 3 shows the flux-weighted centroid velocity $v_{Ly\alpha}$ relative to z_{L1} and the velocity dispersion σ_v. A gradient in $v_{Ly\alpha}$ is evident as one traverses from L2 to L3 through the nebulae ranging from −300 to +800 km s^{-1}. In contrast, the velocity dispersion is roughly constant at $\sigma_v \approx 500$km s^{-1}.

We extract one-dimensional spectra from the final datacube for L1, L2, L1N, L2SW, and L3 through a aperture of 1.7 arcsec^2 (Figure 2(c) and Figure 3(c)). The Lyα emission of L3 is well-modeled by a single Gaussian with central wavelength $\lambda_{L3}^{Ly\alpha} = 4634.9 \pm 0.1$ Å corresponding to $z_{L3} = 2.81259 \pm 0.00008$. The Gaussian model also gives a a velocity dispersion of $\sigma_{L3}^{Ly\alpha} = 150 \pm 6$km s^{-1} (or FWHM$_{L3} = 353 \pm 15$ km s^{-1}).

In Figure 3(c), except for L3, the Lyα emission from the nebula shows both broad and narrow components, confirming the previous long-slit spectra (see also Vernet & Cimatti 2001; Ivison et al. 2010). The nebular emission cannot be well described by a single Gaussian. The figure also emphasizes that L3 is kinematically distinct from the larger nebula; its centroid is offset by several hundred km s^{-1} and it exhibits no broad component.

The Lyα emission spectrum of the nebula also shows evidence for two weak absorption features on both the red and blue sides of the primary emission. Intriguingly, line observations of the CH$^+$ cation, a specific tracer of turbulent dissipation (Falgarone et al. 2017), reveal broad emission lines ascribed to shocks and a broad absorption line (FWHM = 600 km s^{-1}) in the direction of L2SW (E. Falgarone et al. 2019, in preparation). Lyα and CH$^+$ emission of this system both show broad line-emission ascribed to shocks and narrower lines that may imply that L1 and L2 are encompassed by a large and massive HI cloud.

4. Discussion

4.1. Illumination of the Dark Cloud (L3)

In the previous section, we reported on the discovery of L3, a luminous Lyα emitter with an extremely high Lyα equivalent width ($W_{Ly\alpha} > 312$Å) and a FWHM of ≈350km s^{-1}. Cantalupo et al. (2012) reported on a sample of sources with $W_{Ly\alpha} > 240$Å surrounding the ultra-luminous quasar HE0109−3518, which lacks detectable continuum counterparts in deep broadband imaging. They termed these sources "dark galaxies" and argued they were illuminated by the quasar as no star formation could power such high $W_{Ly\alpha}$, i.e., the observed Lyα is fluorescent radiation powered by the incident, ionizing photons. The properties of L3 are consistent with this dark-galaxy scenario, except that the observed UV emission from L1 is orders of magnitude lower than HE0109−3518. Therefore,

[16] SDSS catalog: Alam et al. (2015), Abazajian et al. (2009) *WISE* catalog: Cutri (2012, 2013) 2MASS catalog: Cutri et al. (2003); Skrutskie et al. (2003).
[17] The Pan-STARRS1 Surveys: Chambers et al. (2016) DES DR1: Abbott et al. (2018) DECaLS: http://legacysurvey.org/dr7/.
[18] The definition of "dark galaxy" is defined as a Lyα emitter with rest-frame EW greater than 240 Å, following the definition of Cantalupo et al. (2012).

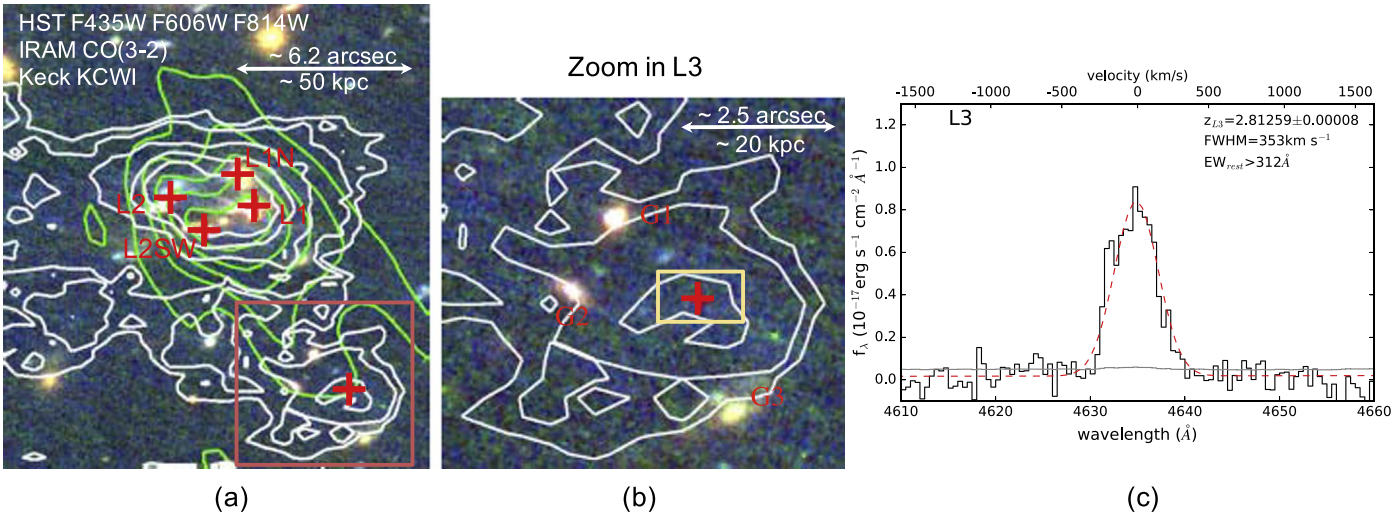

Figure 2. Left panel: a false color *HST* image of SMM J02399 from the Frontier field survey (HST-14038, PI: J. Lotz). We overlay on it KCWI narrow band contours (white) and CO $J = 3$–2 contours (green; Genzel et al. 2003). Middle panel: zoom in on the bright Lyα emitter (L3) marked by red box in the left panel. Right panel: Lyα emission of L3 through the aperture of $\sim$1.7 arcsec^2 ($1\farcs4 \times 1\farcs2$, yellow box in Middle panel). The red dashed line shows a Gaussian fit to the emission profile. The gray line indicates the noise spectrum.

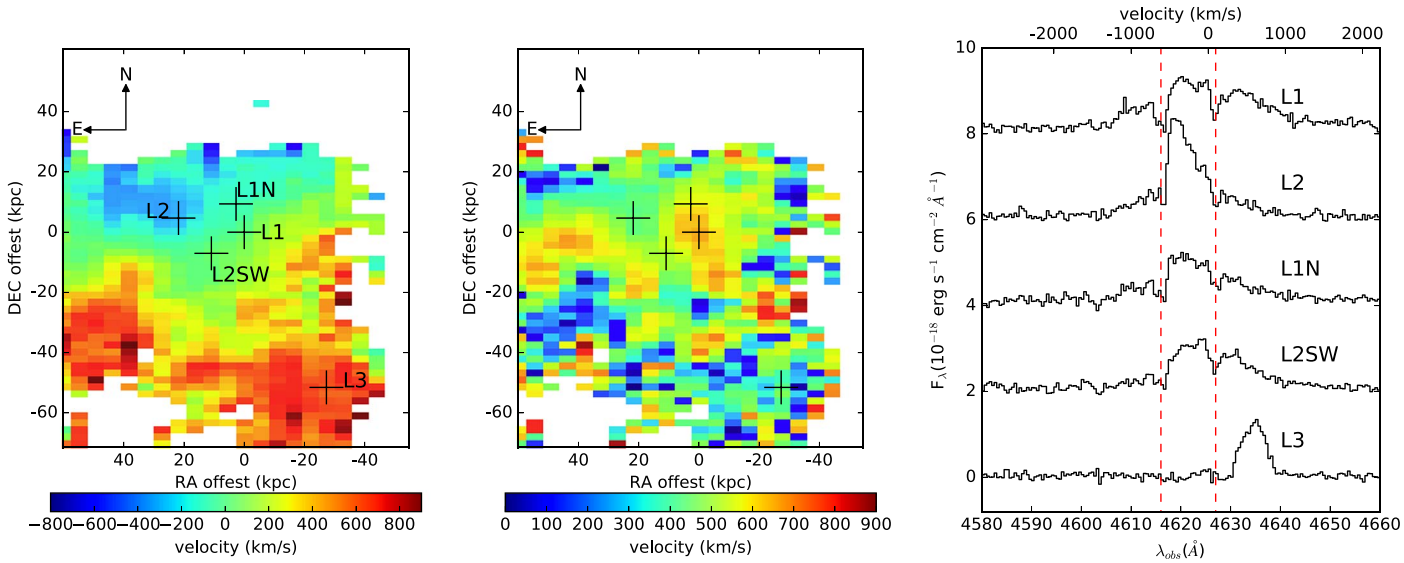

Figure 3. Left panel: flux-weighted velocity-shift map with respect to the systemic redshift of L1, with 3×2 pixels ($1\farcs2 \times 1\farcs4$) in a top-hat filter. Middle panel: velocity dispersion map obtained from the second-moment of the flux distribution. Right panel: spectra at several locations in the system, observed through an aperture of $1\farcs2 \times 1\farcs4$. The spectra are shifted by 2×10^{-18} erg s^{-1} cm^{-2} Å^{-1} for presentation purposes. The vertical red lines are a coherent absorption system.

we propose a scenario wherein the dust-obscured BAL quasar is emitting UV radiation anisotropically, with bright UV emission emitted transverse to our line of sight (Figure 4).

We may test the Lyα fluorescence hypothesis by comparing the observed Lyα flux with that predicted for optically thick gas illuminated by the *unobscured* ionizing radiation of L1. To estimate the unobscured luminosity of L1, consider the following analysis. L1 is detected by the *WISE* satellite with a *W*2 magnitude at $\approx$4.6 μm of 15.2 ± 0.1 mag from ALLWISE source catalog. Adopting the Type-I QSO template from Richards et al. (2006) and scaling to this *W*2 measurement, we may estimate $F_{\nu,LL}$, with ν_{LL} the frequency at the HI Lyman limit. We estimate $L_{\nu,LL}$ of L1 to be $\log_{10}(L_{\nu,LL}/\mathrm{erg\ s^{-1}\ Hz^{-1}}) = 30.07$ and note that this model also reproduces the observed *W*1 flux. In contrast, we estimate the obscured UV luminosity at ν_{LL} along our sightline to be only $\log_{10}(L_{\nu,LL}/\mathrm{erg\ s^{-1}\ Hz^{-1}}) = 27.74$, using the Type-II QSO template from Polletta et al. (2007) and the QSO ultraviolet template from Lusso et al. (2015).

We further assume: (1) the redshift offset between L1 and L3 is due to peculiar motions rather than the Hubble flow, such that the physical separation between the two is comparable to the projected offset; (2) L3 is an optically thick gas cloud with radius of $R_{\mathrm{L3}} \approx 10$ kpc, estimated from the NB image (Figure 1); (3) the optically thick cloud converts a fraction $\eta_{\mathrm{thick}} = 0.66$ of the ionizing photons from the quasar to Lyα photons emitted at a uniform brightness (Gould & Weinberg 1996; Hennawi & Prochaska 2013); (4) L3 is "half-moon" illuminated with a geometric reduction factor of $f_{\mathrm{gm}} = 0.5$ consistent with radiative transfer simulations (Cantalupo et al. 2005; Kollmeier et al. 2010).

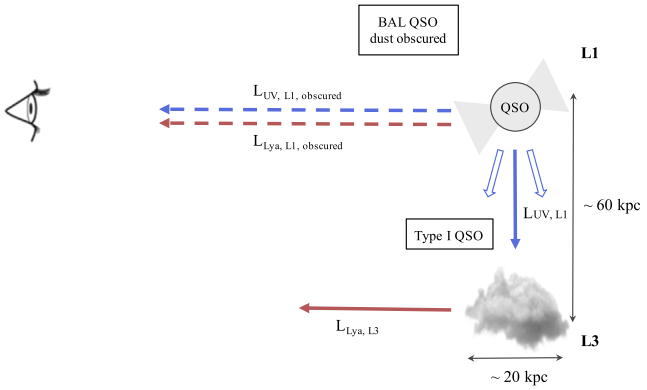

Figure 4. A schematic diagram of the aniostropic emission of L1, illuminating the neighboring, and otherwise dark cloud, L3.

From these assertions, we derive the Lyα surface brightness (Hennawi & Prochaska 2013),

$$\begin{aligned} \mathrm{SB}_{\mathrm{Ly}\alpha} &= \frac{f_{\mathrm{gm}}\,\eta_{\mathrm{thick}}\,h\nu_{\mathrm{Ly}\alpha}}{(1+z)^4}\frac{\Phi}{\pi} \\ &= 5.1\times10^{-17}\left(\frac{1+z}{3.8}\right)^{-4}\left(\frac{f_{\mathrm{gm}}}{0.5}\right)\left(\frac{R}{60\ \mathrm{kpc}}\right)^{-2} \\ &\times\left(\frac{L_{\nu,LL}}{1.2\times10^{30}\,\mathrm{erg\,s^{-1}\,Hz^{-1}}}\right)\mathrm{erg\,s^{-1}\,cm^{-2}\,arcsec^{-2}} \end{aligned} \quad (1)$$

where Φ (phot s^{-1} cm^{-2}) is the ionizing photon number flux, and R is the distance of L3 from L1. Integrating this surface brightness over the observed size of L3, we estimate $f_{\mathrm{L3}}^{\mathrm{Ly}\alpha} = 3.2\times10^{-16}$ erg s^{-1} cm^{-2}. The observed flux of Lyα from L3 is $f_{\mathrm{L3,obs}}^{\mathrm{Ly}\alpha} = 1.8\times10^{-16}$ erg s^{-1} cm^{-2}, corresponding to surface brightness of $\mathrm{SB}_{\mathrm{L3,obs}}^{\mathrm{Ly}\alpha} = 3.0\times10^{-17}$ erg s^{-1} cm^{-2} arcsec^{-2}. This derived value is consistent with the observed flux of Lyα from L3.

Adopting fluorescence as the origin of the Lyα emission, we further estimate a cool gas mass of $M_{\mathrm{cool}} \sim 1.7\times10^{10}M_{\odot}$ using Equation (8) in Cantalupo et al. (2012), assuming a clumping factor $C = 1$ and $T = 2\times10^4$ K. We have also used CLOUDY ionization modeling (Ferland 1996) with the same assumptions above, and found that the best parameter combinations to match $L_{\mathrm{Ly}\alpha,\mathrm{L3}}$ is $(N_{\mathrm{H}}, Z, n_{\mathrm{H}})\sim(10^{22}\ \mathrm{cm^{-2}}, 0.01Z_{\odot}, 0.1\ \mathrm{cm^{-3}})$. Future metal-line observations may provide more precise limits. As the assumed H density of L3 is $\sim$0.1 cm^{-3} according to our best CLOUDY model, the collapse timescale t_{ff} is $\sim1.6\times10^8$ years. Additionally, the cosmic correction t_{ff} from earth is $\sim6.1\times10^8$ years, $\sim$4.5% of the universe age; thus, the "dark matter" t_{ff} will be shorter. The integrated opacity due to Thompson scattering of the ionized cloud is negligible given its very low cross-section (0.665×10^{-24} cm^2) even given our relatively large total electron column density of $N_e \sim 10^{22}$ cm^{-2}. Even a very luminous quasar will give an insignificant flux compared with what we observed.

Numerical studies indicate that the dark-galaxy phase corresponds to gas-rich galaxies prior to efficient star formation (e.g., Francis & Bland-Hawthorn 2004; Cantalupo et al. 2005, 2012; Hennawi et al. 2009; Kollmeier et al. 2010; Marino et al. 2018). A few dedicated dark-galaxy surveys using deep NB imaging and the Multi Unit Spectroscopic Explorer (MUSE; e.g., Cantalupo et al. 2012; Marino et al. 2018) found that the dark clouds reside in the mass range $M_{\mathrm{gas}} \sim 10^{8-10}\,M_{\odot}$, and in the Ly$\alpha$ luminosity range of 10^{41-43} erg s^{-1}. The dark cloud discovered here is consistent with these properties.

Note that there are three galaxies within $5'' \times 5''$ from L3 in the deep *HST* images, which we indicate in panel b of Figure 2 as G1, G2, and G3. The broadband colors of G1 and G3 are consistent with Lyman break galaxies at $z = 3$, though with large uncertainties given the faintness of these galaxies. Even if we allow that G1 and G3 are partially powering L3 and adopt a UV flux from those sources, then the $\mathrm{EW}_{\mathrm{Ly}\alpha}$ estimated for L3 decreases to 209–270 Å. Nevertheless, the Lyα kinematics of L3 has a FWHM of 353 ± 15 km s^{-1}, which is relatively quiescent. Also, the emission peak has a large spatial offset ($\sim2\farcs0$) from both galaxies. These evidences support that L3 is not likely to be powered by either G1 or G3.

Indeed, we cannot rule out a scenario where L3 is powered by gravitational infall, but our current data supports that L3 is more likely to be externally illuminated. Future deep polarimetric observations may rule out such scenarios.

4.2. Lyα Tracing Anisotropic QSO Emission

The dimensions, luminosity, and kinematics of the Lyα nebula surrounding SMM J02399 are reminiscent of the MAMMOTH-1 nebula, which extends to 450 kpc (Cai et al. 2017) and is also powered by a Type-II AGN (Arrigoni Battaia et al. 2018). Cai et al. (2017) argued that the powering mechanism of MAMMOTH-1 could be a combination of photoionization and shocks due to an AGN outflow (e.g., Harrison et al. 2014). SMM J02399 is another nebula hosting a highly obscured system, and may have a similar powering mechanism. For the full nebula around SMM J02399, we measure a total Lyα luminosity of 2.5×10^{44} erg s^{-1} (uncorrected for lensing). The AGN bolometric luminosity is 2.5×10^{46} erg s^{-1} estimated by the UV luminosities (1450 Å) with $L_{\mathrm{bol}} = 4.2\nu L_{\nu}$, 1450 Å (Runnoe et al. 2012). Considered the lensing magnification, the BAL QSO has a similar bolometric luminosity ($\sim10^{46}$ erg s^{-1}) with a normal QSO at $z = 3$. To compare with MAMMOTH-1, we subtracted the Lyα PSF. The PSF is constructed using a full-width-half-maximum that is equal to the seeing of $1\farcs5$. The PSF amplitude is determined from the Lyα luminosity of L1 (in an aperture of $\sim$1.7 arcsec^2) convolved with a Moffat kernel. We find that the central PSF luminosity constitutes only 4.4% of the entire nebula, which is similar to the MAMMOTH-1 measurement of 4%. In the scenario involving collimation, previous studies have already shown that L1 may have a jet/outflow betrayed by the radio morphology, and L2 is likely explained as the shock-excited region or a reflection nebula (Ivison et al. 2010; Frayer et al. 2018). High-resolution CO observations with ALMA and JVLA, and red-sensitive observations of extended and broad metal-line emission (e.g., C$_{\mathrm{IV}}$; Cai et al. 2017) could provide decisive evidence for the outflow scenario.

We note that this Lyα nebula is not the only one that contains multiple embedded galaxies and lacks a clear continuum sources at the peak of the Lyα extended emission. Currently, $\sim$10 Lyα nebulae (also known as Lyα blobs, LAB) are reported as powered by obscured sources. Examples of these are the LABs in Prescott et al. (2012), Bridge et al. (2013), and a few LAB in the SSA22 field (e.g., Matsuda et al. 2004, 2007). With an extent of >140 kpc and a luminosity of 2.5×10^{46} erg s^{-1}, our nebula is one of the largest and most

extended among these systems, and intriguingly hosts the most luminous powering source. Regarding the previous samples of Lyα nebulae and LABs, the SMM J02399 nebula is one of the most luminous discovered to date, and also has multiple components. Also, this is the only system containing a proto-galaxy (a dark galaxy by the definition of Cantalupo et al. 2012), indicating a highly asymmetric ionization.

Figure 4 illustrates the anisotropic emission of ionizing radiation from L1 that we envisage with L1 unobscured in the direction of L3. The UV photons ionize the outer layers of the cool gas cloud to produce Lyα emission. Along our line of sight, it is a typical dust-obscured BAL quasar with substantial foreground absorption, supporting unified models of AGNs. This confirms the primary conclusion from a series of papers that have studied the anisotropic clustering of optically thick gas transverse to and along the line of sight to quasars (e.g., Hennawi & Prochaska 2007, 2013). Based on the same assumption in Section 4.1, here we estimate a lower limit of the open angle of L1 conservatively as $\Omega/4\pi > 0.007$ ($f_{\rm obscured} = 1 - \Omega/4\pi < 0.993$), with the half-angle $\theta > 9.^{\circ}5$. The opening angel is estimated using the linear size of L3 and the distance between L1 and L3, assuming L1 and L3 is at the same redshift, and that the redshift offset is due to the kinematics and not Hubble flow. Further evidence supporting the anisotropic emission hypothesis is the BAL nature of L1, which has been constrained by the moderate continuum polarization with VLT/FORS1 (Vernet & Cimatti 2001). BAL QSOs are expected to radiate as Type-I QSOs only through patches free of dust and dense outflowing gas (e.g., Ogle et al. 1999). On the other hand, the SMG (L2SW) close to L1 also can be a plausible source to illuminate L3, the dust cocoon of which may not necessarily be homogeneous.

5. Concluding Remarks

In this paper, we present the Keck/KCWI IFU observations of a Lyα blob powered by SMM J02399 at $z \sim 2.8$. With KCWI, we discover a dark cloud that we argue is illuminated by the dust-obscured QSO of the system. This implies strong, anisotropic UV radiation from the QSO, which was also suggested by previous polarimetry observations. The future red/blue-sensitive IFS, Keck Cosmic Reionization Mapper (KCRM)/KCWI can further reveal the properties and kinematics of other lines, such as Lyβ, He II, C IV, to further reveal the nature of this and similar systems. We are also pursuing a KCWI survey of Type-II AGN to study the population of Lyα nebulae in a set of fully obscured sources.

This work was supported by National Key Program for Science and Technology Research and Development (grant 2016YFA0400703) and the National Science Foundation of China (11721303). We are thankful for the support from the National Science Foundation of China (NSFC) grants No. 11373008, 11533001. Q.L. gratefully acknowledges financial support from China Scholarship Council. Z.C. acknowledges the supports provided by NASA through the Hubble Fellowship grant HST-HF2-51370 awarded by the Space Telescope Science Institute, which is operated by the Association of Universities for Research in Astronomy, Inc., for NASA, under contract NAS 5-26555. E.F. gratefully acknowledges funding from the European Research Council, under the European Community's Seventh framework Programme, through the Advanced Grant MIST (FP7/2017-2022, No. 742719). S.C. gratefully acknowledges support from Swiss National Science Foundation grant PP00P2_163824. The data presented herein were obtained at the W. M. Keck Observatory, which is operated as a scientific partnership among the California Institute of Technology, the University of California, and the National Aeronautics and Space Administration. The Observatory was made possible by the generous financial support of the W. M. Keck Foundation.

ORCID iDs

Qiong Li https://orcid.org/0000-0002-3119-9003
Zheng Cai https://orcid.org/0000-0001-8467-6478
J. Xavier Prochaska https://orcid.org/0000-0002-7738-6875
Fabrizio Arrigoni Battaia https://orcid.org/0000-0002-4770-6137
R. J. Ivison https://orcid.org/0000-0001-5118-1313
Sebastiano Cantalupo https://orcid.org/0000-0001-5804-1428
James Don Neill https://orcid.org/0000-0002-0466-1119
Ran Wang https://orcid.org/0000-0003-4956-5742

References

Abazajian, K. N., Adelman-McCarthy, J. K., Agüeros, M. A., et al. 2009, ApJS, 182, 543
Abbott, T. M. C., Abdalla, F. B., Allam, S., et al. 2018, ApJS, 239, 18
Alam, S., Albareti, F. D., Allende Prieto, C., et al. 2015, ApJS, 219, 12
Antonucci, R. 1993, ARA&A, 31, 473
Arrigoni Battaia, F., Chen, C.-C., Fumagalli, M., et al. 2018, A&A, 620, A202
Arrigoni Battaia, F., Prochaska, J. X., Hennawi, J. F., et al. 2018, MNRAS, 473, 3907
Bridge, C. R., Blain, A., Borys, C. J. K., et al. 2013, ApJ, 769, 91
Cai, Z., Fan, X., Yang, Y., et al. 2017, ApJ, 837, 71
Cantalupo, S., Arrigoni-Battaia, F., Prochaska, J. X., Hennawi, J. F., & Madau, P. 2014, Natur, 506, 63
Cantalupo, S., Lilly, S. J., & Haehnelt, M. G. 2012, MNRAS, 425, 1992
Cantalupo, S., Porciani, C., Lilly, S. J., & Miniati, F. 2005, ApJ, 628, 61
Chambers, K. C., Magnier, E. A., Metcalfe, N., et al. 2016, arXiv:1612.05560
Cutri, R. M., Skrutskie, M. F., van Dyk, S., et al. 2003, yCat, 2246
Cutri, R. M. 2012, yCat, 2311
Cutri, R. M. 2013, yCat, 2328
Falgarone, E., Zwaan, M. A., Godard, B., et al. 2017, Natur, 548, 430
Ferland, G. J. 1996, Hazy, A Brief Introduction to Cloudy 90 University of Kentucky Internal Report (Lexington, KY: Univ. Kentucky), 565
Francis, P. J., & Bland-Hawthorn, J. 2004, MNRAS, 353, 301
Frayer, D. T., Ivison, R. J., Scoville, N. Z., et al. 1998, ApJL, 506, L7
Frayer, D. T., Maddalena, R. J., Ivison, R. J., et al. 2018, ApJ, 860, 87
Fumagalli, M., Prochaska, J. X., Kasen, D., et al. 2011, MNRAS, 418, 1796
Genzel, R., Baker, A. J., Tacconi, L. J., et al. 2003, ApJ, 584, 633
Gould, A., & Weinberg, D. H. 1996, ApJ, 468, 462
Haiman, Z., & Rees, M. J. 2001, ApJ, 556, 87
Harrison, C. M., Alexander, D. M., Mullaney, J. R., & Swinbank, A. M. 2014, MNRAS, 441, 3306
Heckman, T. M., Lehnert, M. D., Miley, G. K., & van Breugel, W. 1991, ApJ, 381, 373
Hennawi, J. F., & Prochaska, J. X. 2007, ApJ, 655, 735
Hennawi, J. F., & Prochaska, J. X. 2013, ApJ, 766, 58
Hennawi, J. F., Prochaska, J. X., Cantalupo, S., & Arrigoni-Battaia, F. 2015, Sci, 348, 779
Hennawi, J. F., Prochaska, J. X., Kollmeier, J., & Zheng, Z. 2009, ApJL, 693, L49
Ivison, R. J., Smail, I., Le Borgne, J.-F., et al. 1998, MNRAS, 298, 583
Ivison, R. J., Smail, I., Papadopoulos, P. P., et al. 2010, MNRAS, 404, 198
Kennicutt, R. C., & Evans, N. J. 2012, ARA&A, 50, 531
Kollmeier, J. A., Zheng, Z., Davé, R., et al. 2010, ApJ, 708, 1048
Lusso, E., Worseck, G., Hennawi, J. F., et al. 2015, MNRAS, 449, 4204
Marino, R. A., Cantalupo, S., Lilly, S. J., et al. 2018, ApJ, 859, 53
Matsuda, Y., Iono, D., Ohta, K., et al. 2007, ApJ, 667, 667
Matsuda, Y., Yamada, T., Hayashino, T., et al. 2004, AJ, 128, 569

Matsuda, Y., Yamada, T., Hayashino, T., et al. 2011, MNRAS, 410, L13
Morrissey, P., Matuszewski, M., Martin, C., et al. 2012, Proc. SPIE, 8446, 844613
Nenkova, M., Sirocky, M. M., Ivezić, Ž., & Elitzur, M. 2008, ApJ, 685, 147
Ogle, P. M., Cohen, M. H., Miller, J. S., et al. 1999, ApJS, 125, 1
Polletta, M., Tajer, M., Maraschi, L., et al. 2007, ApJ, 663, 81
Prescott, M. K. M., Dey, A., Brodwin, M., et al. 2012, ApJ, 752, 86
Prochaska, J. X., & Hennawi, J. F. 2009, ApJ, 690, 1558
Rees, M. J. 1988, MNRAS, 231, 91
Richards, G. T., Lacy, M., Storrie-Lombardi, L. J., et al. 2006, ApJS, 166, 470
Runnoe, J. C., Brotherton, M. S., & Shang, Z. 2012, MNRAS, 422, 478
Skrutskie, M. F., Cutri, R. M., Stiening, R., et al. 2003, yCat, 7233
Tristram, K. R. W., Meisenheimer, K., Jaffe, W., et al. 2007, A&A, 474, 837
Vernet, J., & Cimatti, A. 2001, A&A, 380, 409
Villar-Martín, M., Binette, L., & Fosbury, R. A. E. 1999a, A&A, 346, 7
Villar-Martín, M., Fosbury, R. A. E., Binette, L., Tadhunter, C. N., & Rocca-Volmerange, B. 1999b, A&A, 351, 47
Villar-Martín, M., Sánchez, S. F., Humphrey, A., et al. 2007, MNRAS, 378, 416